European Journal of Human Genetics (2021) 29:816–826
https://doi.org/10.1038/s41431-020-00804-7

ARTICLE

Novel variants in *TUBA1A* cause congenital fibrosis of the extraocular muscles with or without malformations of cortical brain development

Julie A. Jurgens[1,2,3,4] · Brenda J. Barry[2,5] · Gabrielle Lemire[6] · Wai-Man Chan[1,2,3,4,5] · Mary C. Whitman[1,7,8] · Sherin Shaaban[1,2,3,9] · Caroline D. Robson[10,11] · Sarah MacKinnon[7,8] · Eleina M. England[12,13,14] · Hugh J. McMillan[15] · Christopher Kelly[16] · Brandon M. Pratt[1,2,3] · Care4Rare Canada Consortium · Anne O'Donnell-Luria[12,13,14] · Daniel G. MacArthur[12,13,17,18] · Kym M. Boycott[6,19] · David G. Hunter[7,8] · Elizabeth C. Engle[1,2,3,4,5,7,8]

Received: 13 October 2020 / Revised: 12 December 2020 / Accepted: 17 December 2020 / Published online: 1 March 2021

Abstract

Variants in multiple tubulin genes have been implicated in neurodevelopmental disorders, including malformations of cortical development (MCD) and congenital fibrosis of the extraocular muscles (CFEOM). Distinct missense variants in the beta-tubulin encoding genes *TUBB3* and *TUBB2B* cause MCD, CFEOM, or both, suggesting substitution-specific mechanisms. Variants in the alpha tubulin-encoding gene *TUBA1A* have been associated with MCD, but not with CFEOM. Using exome sequencing (ES) and genome sequencing (GS), we identified 3 unrelated probands with CFEOM who harbored novel heterozygous *TUBA1A* missense variants c.1216C>G, p.(His406Asp); c.467G>A, p.(Arg156His); and c.1193T>G, p.(Met398Arg). MRI revealed small oculomotor-innervated muscles and asymmetrical caudate heads and lateral ventricles with or without corpus callosal thinning. Two of the three probands had MCD. Mutated amino acid residues localize either to the longitudinal interface at which α and β tubulins heterodimerize (Met398, His406) or to the lateral interface at which tubulin protofilaments interact (Arg156), and His406 interacts with the motor domain of kinesin-1. This series of individuals supports *TUBA1A* variants as a cause of CFEOM and expands our knowledge of tubulinopathies.

Introduction

Neurodevelopment is facilitated by the assembly or disassembly of cytoskeletal proteins called microtubules (MTs), which facilitate neuronal migration and axon growth [1]. MTs are composed of two major families of tubulins, α and β, which heterodimerize to form longitudinal polymers, or protofilaments [2]. Thirteen protofilaments interact laterally to form an MT [3]. MTs are dynamic, and heterodimers are added or removed to promote MT elongation or contraction [4]. Alpha (α) and beta (β) tubulin families are made up of multiple isotypes, each encoded by a specific gene [5]. Variants in genes encoding both α and β tubulin isotypes result in disorders called tubulinopathies [6], of which two forms include various malformations of cortical brain development (MCD; HP:0032059) [7] and/or congenital fibrosis of the extraocular muscles (CFEOM; HP:0001491).

CFEOM is characterized by congenital ptosis (HP:0007911) and non-progressive restriction of vertical eye movement, with variable restrictions of horizontal eye movement. In humans with CFEOM, the superior division of the oculomotor nerve (CN III) and its targets, the superior rectus and levator palpebrae superioris muscles, are severely hypoplastic, while the abducens nerve and inferior division of CN III and their muscle targets are variably hypoplastic [8–10]. CFEOM can be isolated or accompanied by other symptoms and can result from heterozygous missense

Members of the Care4Rare Canada Consortium are listed in the Supplementary Information.

Supplementary information The online version of this article (https://doi.org/10.1038/s41431-020-00804-7) contains supplementary material, which is available to authorized users.

✉ Elizabeth C. Engle
elizabeth.engle@childrens.harvard.edu

Extended author information available on the last page of the article

variants in the MT-associated kinesin-encoding gene *KIF21A* (MIM#608283) [11], in the β tubulin-encoding gene *TUBB3* (MIM#602661), and rarely in other genes including the β tubulin-encoding gene *TUBB2B* (MIM#612850) [12–16].

MCDs arise from defective development of the cerebral cortex and are often associated with developmental delays (HP:0012758), intellectual disabilities (HP:0001249), and seizures (HP:0001250). Variants in multiple tubulin-encoding genes including *TUBA1A* (MIM#602529) have been implicated in MCD without CFEOM (MIM#611603) [17]. By contrast, *TUBB2B* variants can cause MCD with or without CFEOM (MIM#610031) [15, 18], and *TUBB3* variants can cause MCD (MIM#614039), CFEOM (MIM#600638), or both [13, 16, 19].

Human tubulin variants causing MCD or CFEOM are heterozygous, missense, and sometimes recurrent, supporting an etiology that is distinct from loss of function. Consistent with this, loss of *Tubb3* in mice does not cause a developmental phenotype, and loss of *Tubb2a* or *Tubb2b* causes mild MCD [20, 21]. *TUBA1A* is expressed highly in the brain, and mice with missense variants in or knockout of *Tuba1a* have MCD or other brain malformations that are often perinatal lethal [21–24]. While *TUBA1A* variants are frequently reported to cause strabismus (HP:0000486) and more rarely reported to affect cranial nerve development [25], no humans or mice with *TUBA1A/ Tuba1a* variants have been reported to have CFEOM. Here, we report heterozygous *TUBA1A* missense variants in three unrelated probands who have CFEOM with or without MCD.

Individuals and methods

Consent and clinical data collection

Studies were performed in accordance with the Declaration of Helsinki. Families were consented into a research protocol approved by the Institutional Review Board of Boston Children's Hospital, Boston, MA. Individual 3 was also consented into the Care4Rare Canada Research Program approved by the Children's Hospital of Eastern Ontario Research Ethics Board. Clinical data were obtained through retrospective review of clinical records along with questionnaires and clinical updates provided by each family. Individuals 1 and 2 were also seen in the Congenital Cranial Dysinnervation Disorders (CCDD) clinic at Boston Children's Hospital. Brain magnetic resonance images (MRI) were obtained clinically and reviewed retrospectively. When possible, clinical features were standardized using Human Phenotype Ontology [7]. Head circumference percentile and z-score for Individual 3 is based on the Nellhaus scale [26]. All other height, weight, and head circumference percentiles and z-scores were obtained from the United States Centers for Disease Control and Prevention, National Center for Health Statistics. CDC growth charts: United States (http://www.cdc.gov/growthcharts/. May 30, 2000).

Sample collection and DNA sequencing

Family 1: DNA was extracted from saliva of the probands and parents using prepIT.L2P solution (DNA Genotek, Ottawa, ON, Canada). Sanger sequencing of coding exons and splice junctions of *TUBB3*, *TUBB2B*, *CHN1*, *PHOX2A*, and *MYF5* and of *KIF21A* exons 8, 20, and 21 was uninformative. Genome sequencing (GS) of the trio was conducted at Baylor College of Medicine Human Genome Sequencing Center (Houston, TX) as part of NIH Gabriella Miller Kids First Research Program. DNA libraries were prepared using KAPA Hyper PCR-free library prep kit (KAPA Biosystems Inc., Wilmington, MA) and sequenced on an Illumina HiSeq X to 30X mean coverage using 150 bp paired-end reads. Raw data were transferred to the Broad Institute of MIT and Harvard for alignment to the human reference genome (https://www.ncbi.nlm.nih.gov/grc; GRCh38) by BWA-MEM and reprocessing by Picard (https://broadinstitute.github.io/picard/) [27]. Joint variant calling was conducted with GATK 4.0 HaplotypeCaller alongside >20,000 reference genomes at the Broad Institute [28]. Filtering was conducted using GATK Variant Quality Score Recalibrator. Variants were annotated with a custom version of Ensembl Variant Effect Predictor [29] and uploaded to seqr for analysis (https://seqr.broadinstitute.org/).

Family 2: DNA was extracted from saliva of the proband and parents as described for Family 1. Sanger sequencing of coding regions and splice junctions of *TUBB3*, *TUBB2B, CHN1*, *PHOX2A* and *KIF21A* was uninformative. Exome sequencing (ES) of the trio was performed at the Ocular Genomics Institute (OGI, Massachusetts Eye and Ear Infirmary, Boston, MA). Libraries were prepared using the Agilent SureSelect Human v4 kit and sequenced on an Illumina HiSeq 2000. 99% of captured regions had ≥10X coverage. Additional data was processed as for Family 1.

Family 3: DNA was extracted from blood of the proband only and ES was performed as part of the Care4Rare Canada Research Program [30]. Targeted exon capture was performed using the Agilent SureSelect Human All Exon 50 Mb (v5) enrichment kit and sequenced on an Illumina HiSeq 2000 using 2 × 100 bp chemistry. Alignment, variant calling, and annotation were done with a bcbio-based pipeline (https://github.com/bcbio/bcbio-nextgen), GEMINI [31], methods accumulated in FORGE and Care4Rare

Canada Projects [30, 32], and custom annotation scripts (https://github.com/naumenko-sa/cre).

ES/GS analysis

For Individuals 1 and 2, ExAC v0.3 [33], gnomAD r2.0.2 [34], TOPMed (https://bravo.sph.umich.edu/freeze5/hg38/), and 1000 Genomes Project Phase 3 [35] were used as reference populations. *De novo* heterozygous variants with minor allele frequency (MAF) < 0.001 and homozygous or compound heterozygous variants with MAF < 0.01 were identified. Hemizygous X-linked variants with MAF < 0.001 were also identified for Individual 2. All variants were excluded if observed in homozygosity in reference population(s), and *de novo* variants were deprioritized if seen in >5 individuals in reference population(s). Variants that passed QC filters and had allele balances >15 and genotype qualities >20 were selected, and indels and missense, nonsense, or splice site-altering single nucleotide variants were prioritized. Variants were manually inspected in Integrative Genomics Viewer and deprioritized if they had poor allele balance or variant quality, low read depth, local mapping errors, indel stutter, strand bias, or mismatched reads. Variants were excluded if common (MAF > 0.05) in an internal database of rare disease samples from the Broad Institute. *De novo* variants were deprioritized if observed in other individuals with disparate phenotypes in the internal rare disease database.

For Individual 3, ES was analyzed for autosomal or X-linked heterozygous, homozygous, or putative compound heterozygous variants with MAF < 0.001 in gnomAD r2.0.2 [34]. Indels and missense, nonsense, or splice site-altering single nucleotide variants were prioritized. Heterozygous and X-linked variants seen <7 times or compound heterozygous and homozygous variants seen <15 times out of 5220 alleles in an internal database of rare disease samples from the Care4Rare Canada Project were selected.

Sanger validation and cosegregation analysis

PCR primers were designed for Sanger validation of *TUBA1A* variants in all three families and cosegregation analysis in families 1 and 2 (Supplementary Table 1).

Database sharing of variants

Individuals and their *TUBA1A* variants were deposited in the Global Variome shared LOVD (https://databases.lovd.nl/shared/genes/TUBA1A; individual ID numbers 00311884, 00311881, and 00311893) and ClinVar (accession numbers SCV001449530-SCV001449532; https://www.ncbi.nlm.nih.gov/clinvar/) [36].

Protein structural modeling

Using PyMOL (Molecular Graphics System v2.2.2, Schrödinger, LLC), residues were mapped to structures of the MT with EB3 (PDB:3JAK) [37] and α/β tubulins with kinesin-1 (PDB:4HNA) [38]. Polar contacts within 5 Å were identified. 2D mapping of *TUBA1A*-CFEOM residues was performed (Supplementary Fig. 2).

Tubulin multiple sequence alignment

Multi-sequence alignment was performed using Clustal Omega v1.2.4 [39] (date of access: December 7, 2020) and visualized using Jalview v2.11.13 [40] (Supplementary Fig. 3).

Results

Clinical findings

Each individual had bilateral congenital ptosis (HP:0007911), restricted vertical eye movements and variably restricted horizontal eye movements diagnostic of CFEOM (HP:0001491; Fig. 1A-E). Individuals 1 and 2 also had abnormal conjugate eye movements (HP:0000549) with convergence on attempted upgaze (Fig. 1A) and anomalous extraocular muscle insertions at surgery, which are common findings in CFEOM [41]. Individual 3 had learning disabilities (HP:0001328), cognitive delays (HP:0100543) and behavioral challenges (HP:0007018; HP:0010865); Individual 1 had mild learning disability (HP:0001328); and Individual 2 had normal intellectual and social development. Individual 3 had gross motor delays (HP:0002194) while Individual 2 had mild clumsiness. Individual 3 had cyclic vomiting (HP:0002572). Additional clinical features are presented in Table 1, Supplementary Text 1, and Supplementary Table 3.

The oculomotor nerves and extraocular muscles could be visualized on MRI scans of Individual 1; the nerves appeared hypoplastic bilaterally and the superior and medial rectus muscles appeared small, but imaging prevented clear visualization (Fig. 1F, G). Individuals 1 and 3 had bilateral perisylvian polymicrogyria (HP:0032407; Fig. 2D-F, O, P). Though Individual 2 had no detectable MCD (Fig. 2J), deficiency of the falx cerebri (HP:0010654) resulting in interdigitating frontal lobes, a finding of unclear clinical significance, was observed (Fig. 2K). MRI scans of each of the individuals revealed asymmetry of the caudate heads (HP:0002339) and lateral ventricles (HP:0030047; Fig. 2B-C, H-I, M-N). Individual 1 also had deficiency of the rostrum of the corpus callosum (Fig. 2A), while Individuals 2 and 3 had thinning of the body and splenium or posterior

Fig. 1 *TUBA1A* variants are associated with CFEOM. A–I Five positions of gaze in Individual 1 prior to her first strabismus surgery at 2.5 years of age, demonstrating ophthalmic features consistent with CFEOM. The individual's eye movements were directed as follows: (**A**) up; (**B**) right; (**C**) forward; (**D**) left; (**E**) down. Notable ophthalmic features include: (**A**) bilateral limitations of upgaze and convergence on attempted upgaze; (**C**) Bilateral ptosis and primary eye position in downgaze; (**B**, **D**): full horizontal eye movements; (**E**): mild bilateral limitations of downgaze and preferred chin-up head positioning. **F** Axial T2 weighted MR image (2 mm/0 mm gap thickness) at the level of the interpeduncular and suprasellar cisterns faintly demonstrates the oculomotor nerves (arrows). Although the slice thickness was not optimized for cranial nerve imaging, these nerves appear hypoplastic. **G** Coronal T1 MPRAGE image (0.9 mm/0 mm gap thickness) through the orbits demonstrates small superior and medial rectus muscles bilaterally (arrows).

body of the corpus callosum, respectively (HP:0002079; Fig. 2G, L). The olfactory sulci and bulbs, internal capsules, cerebellum, and brainstem appeared normal in all three individuals. MRI findings are summarized in Table 1.

Sequencing results

Candidate variants in multiple genes were detected after filtering (Supplementary Table 2). ES/GS identified heterozygous *TUBA1A* variants c.1216C > G, p.(His406Asp) (Individual 1); c.467G > A, p.(Arg156His) (Individual 2); and c.1193T > G, p.(Met398Arg) (Individual 3); all annotated with transcript NM_006009.4. Variants occurred at conserved residues [42], were absent from population databases, and were predicted to be damaging [43] (Table 1). All variants were classified as pathogenic or likely pathogenic for established *TUBA1A*-associated phenotypes by ACMG guidelines [44]. Sanger sequencing validated the presence of *TUBA1A* variants in all three probands and absence in unaffected parents and siblings of Individuals 1 and 2 (Supplementary Fig. 1). *TUBA1A* is highly conserved across species and is ranked as the 57th most missense constrained gene within humans among 19,704 total genes tested (missense $z = 5.584$) [45].

Protein structural modeling

Representative lateral and longitudinal tubulin interfaces are represented in Fig. 3A. His406 and Met398, substituted to aspartate and arginine in Individuals 1 and 3, respectively, are in α helix H11 on the MT surface (Fig. 3B). These residues are near to the longitudinal interface between α and β tubulin within a heterodimer, but neither residue is recognized to participate in bonded contacts (Fig. 3C) [46]. MCD-associated residues are also in this region (Fig. 3B) [25]. Like certain β tubulin-associated CFEOM residues, His406 is predicted to interact with the kinesin-1 motor domain (Fig. 3D) [38]. p.(Arg156His) identified in Individual 2 is in α-helix H4 [47] near the interface for lateral contacts with adjacent protofilaments (Fig. 3E). A p.(Arg156Gly) substitution has been reported in an individual with MCD and epilepsy but without CFEOM [48], and other substitutions causing MCD have been reported in α-helix H4 (Fig. 3B) [49].

Discussion

The three probands had CFEOM (HP:0001491) with or without variable neurodevelopmental disability. MRIs were consistent with classic tubulinopathies, including asymmetry of the caudate heads (HP:0002339) and lateral ventricles (HP:0030047) with abnormalities of the corpus callosum in all three individuals (HP:0002079), MCD in Individuals 1 and 3 (HP:0032059), and oculomotor nerve and extraocular muscle findings consistent with CFEOM in Individual 1. Unlike individuals with more severe presentation of CFEOM and neurodevelopmental delays and/or MCD due to *TUBB3* variants, each participant in this series had normal appearing anterior commissure, olfactory system, cerebellum, and brainstem. Each proband harbored a novel *TUBA1A* heterozygous variant that is predicted to be damaging (p.(Arg156His), p.(Met398Arg), or p.(His406Asp)). Notably, a proband with a *TUBA1A* p.(Gly59Ser) variant was previously reported to have eyelid asymmetry and a unilateral deficit of ocular elevation upon adduction in the absence of MCD, and a proband with a *TUBA1A* p.(Arg390His) variant was reported to have ptosis (HP:0000508), strabismus (HP:0000486), and nystagmus (HP:0000639) in the absence of MCD [50]. These phenotypes may also be CFEOM, but

Table 1 Summary of *TUBA1A* variants and clinical features.

	Individual 1	Individual 2	Individual 3
Sex	Female	Male	Female
Geographic location/ Ethnicity	USA, Hispanic	USA, Caucasian/Hispanic	French Canadian, Caucasian
Variant genomic location (GRCh38/ hg38)	chr12:49185150G>C	chr12:49185899C>T	chr12:49185173 A>C
Variant (cDNA, protein; transcript NM_006009.4)	c.1216C>G, p.(His406Asp)	c.467G > A, p.(Arg156His)	c.1193T>G, p.(Met398Arg)
Exon	4	4	4
Inheritance	*De novo*	*De novo*	Unknown
Method of variant identification	GS	ES	ES
Sanger validated?	Y	Y	Y
Properties of amino acid residues (WT> Predicted Variant)	Polar basic>Polar acidic	Polar basic>Polar basic	Nonpolar>Polar basic
PhyloP score [41, 42][a]	7.76	1.91	7.32
PHRED-scaled CADD score [43][b]	26.7	23.8	27.6
ACMG Classification [44][c]	Pathogenic	Likely pathogenic	Likely pathogenic
Age at clinical presentation	Infancy	Infancy	Infancy
Current age	13 years	13 years	11 years
Ophthalmological features			
Ophthalmological diagnosis of CFEOM (HP:0001491)	Y	Y	Y
Bilateral congenital ptosis (HP:0007911)	Y	Y (right > left)	Y
Impaired ocular abduction (HP:0000634)	N	Y, bilateral (mild)	Y, bilateral
Impaired ocular adduction (HP:0000542)	N	N	Y, bilateral
Limited vertical eye movements	Y, limited upgaze and mildly limited downgaze bilaterally	Y, limited upgaze bilaterally	Y, limited upgaze and downgaze bilaterally
Compensatory head posture (HP:0031705)	Y, Chin-up head positioning	Y, Chin-up head positioning	N
Abnormal conjugate eye movement (HP:0000549)	Y, convergence on attempted upgaze, divergence and occasional convergence on attempted downgaze	Y, convergence on attempted upgaze with secondary pseudo-convergence contraction nystagmus, left-side synkinetic movement of eyelid	N
Anomalous extraocular muscle insertions	Y, of left superior oblique muscle	Y, of right inferior rectus muscle	N
Horizontal nystagmus (HP:0000666)	N	N	Y, bilateral
Ophthalmological surgeries	Y, bilateral	Y, bilateral	Y, bilateral

Table 1 (continued)

	Individual 1	Individual 2	Individual 3
Development			
Delayed speech and language development (HP:0000750)	Y, mild early delays	N	Y, mild early delays
Delayed fine motor development (HP:0010862)	N	Y, mild early delays	Y
Delayed gross motor development (HP:0002194)	N	Y, mild early delays	Y
Learning disability (HP:0001328)	Y, but no formal diagnosis	N	Y, but no formal diagnosis
Cognitive impairment (HP:0100543)	N	N	Delays but no formal diagnosis
Attention deficit hyperactivity disorder (HP:0007018)	N	N	Y
Oppositional defiant disoder (HP:0010865)	N	N	Y
Exam-age	2 years and 7 months	2 years and 7 months	10 years and 10 months
Height	88 cm (18th percentile, z=−0.92)	90.2 cm (28th percentile; z=−0.57)	146.3 cm (68.2 percentile, z = 0.44)
Weight	13.8 kg (67th percentile, z = 0.44)	12.587 kg (24th percentile, z=−0.72)	31.5 kg (22nd percentile, z=−0.61)
Head circumference	50 cm (89th percentile, z = 1.21)	48.9 cm (39th percentile, z=−0.28)	50.7 cm (9th percentile, z=−1.3, Nellhaus Scale)
Dysphagia (HP:0002015)	N	None diagnosed, but some choking on solid food	N
Ankyloglossia (HP:0010296)	N	Y, relieved with tongue release surgery	N
Thickened ears (HP:0009894)	N	N	Y
Small forehead (HP:0000350)	N	N	Y
Deeply set eyes (HP:0000490)	N	N	Y
Infantile muscular hypotonia (HP:0008947)	Y	N	Y
Achilles tendon contracture (HP:0001771)	N	N	Y
Unsteady gait (HP:0002317)	N	N	Y
Tip-toe gait (HP:0030051)	N	N	Y

Table 1 (continued)

	Individual 1	Individual 2	Individual 3
Additional features			
Cyclic/episodic vomiting (HP:0002572)	N	N	Y
Gastrointestinal dysmotility (HP:0002579)	N	N	Y
Gastroesophageal reflux (HP:0002020)	N	Y	N
Brain MRI findings			
Bilateral perisylvian polymicrogyria (HP:0032407)	Y	N	Y
Aplasia of the falx cerebri (HP:0010654)	N	Y, slightly interdigitating frontal lobes	N
Hypoplasia of the corpus callosum (HP:0002079)	Y	Y	Y
Abnormality of the anterior commissure (HP:0030301)	Slightly enlarged	N	N
Abnormality of lateral ventricle (HP:0030047)	Y, asymmetry	Y, asymmetry	Y, asymmetry
Abnormal caudate nucleus morphology (HP:0002339)	Y, asymmetry of caudate heads	Y, asymmetry of caudate heads	Y, asymmetry of caudate heads
Abnormality of brainstem morphology (HP:0002363)	N	Possible slightly obtuse angle between the pons/medulla	N
Abnormality of the extraocular muscles (HP:0008049)	Y, superior rectus muscles very small, medial rectus muscles small bilaterally	Y, superior rectus muscles and medial rectus muscles small bilaterally	NA

Y yes, *N* no, *NA* not ascertainable/unknown, *ES* exome sequencing, *GS* genome sequencing, *CFEOM* congenital fibrosis of the extraocular muscles.

[a]phyloP100way from PHASTv1.5, date of access: November 27, 2020.

[b]CADDv1.6, date of access: November 27, 2020.

[c]Variants were classified using ACMG criteria (Richards et al., 2015) in November of 2020. These criteria are not applicable for novel gene identification and have limited utility for significant novel phenotype expansion. Classification is provided for established TUBA1A-associated tubulinopathy phenotypes, but excludes novel phenotype expansions (e.g., CFEOM) which are not yet well established in association with *TUBA1A* variants.

were not reported as such. Furthermore, in an amino acid multi-sequence alignment, TUBA1A-Arg390 corresponds to the reported CFEOM residue TUBB3-Arg380 [13], supporting the possible association of this residue with CFEOM (Supplementary Fig. 3). Thus, variants in the MCD-associated gene *TUBA1A* can cause CFEOM with or without concurrent MCD, and *TUBA1A* should be included in genetic testing panels for individuals who have CFEOM and other features of tubulinopathies.

Ocular motility phenotypes are frequently reported in tubulinopathies. In a recent study, strabismus (HP:0000486) was a feature in 18/29 individuals (62%) with *TUBA1A*-associated tubulinopathies, of whom 4 also had nystagmus (HP:0000639) [25]. It is likely that most of these individuals have comitant strabismus (HP:0025069), which is common in the general population and is characterized by a constant degree of ocular misalignment regardless of the direction of gaze. CFEOM is a form of incomitant strabismus

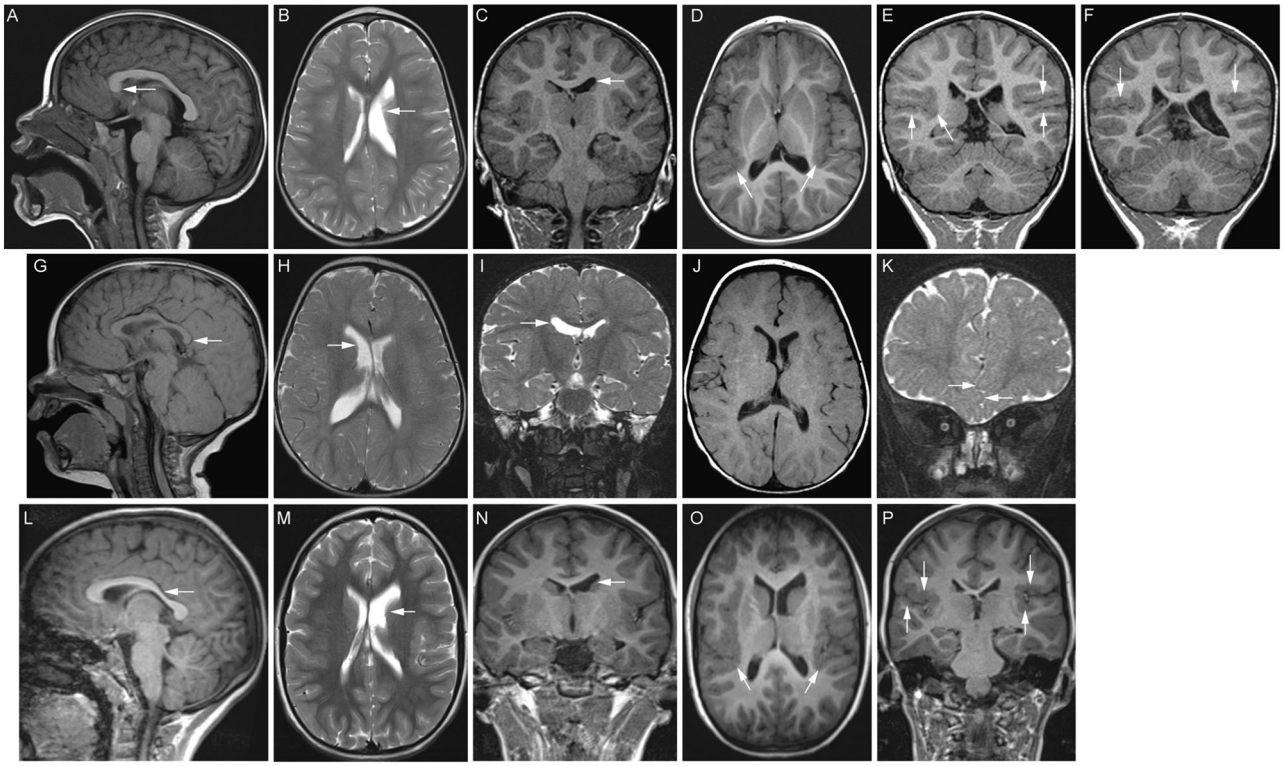

Fig. 2 Brain MRI demonstrates features of classic tubulinopathies with or without MCD. A–F MR images from Individual 1 at 20 months of age. **A** Midline sagittal T1 FLAIR MR image reveals deficiency of the rostrum of the corpus callosum. **B** Axial T2 and (**C**) coronal T1 MPRAGE MR images demonstrate an asymmetrically smaller, foreshortened body of the left caudate nucleus (white arrows) with mild prominence and dysmorphism of the ipsilateral lateral ventricle. **D** Axial T1 FLAIR MR image (5 mm/2.25 mm gap thickness) demonstrates thickening and irregularity of the posterior perisylvian cortex (white arrows), most pronounced on the right. **E**, **F** Coronal T1 MPRAGE MR images (0.9 mm/0 mm gap thickness) confirm bilateral perisylvian polymicrogyria (white arrows). **G–I** MR images from Individual 2 at 13 months of age. **G** 1.5T Siemens Symphony midline sagittal T1 MR image (4 mm/0.8 mm gap thickness) reveals mild thinning of the body and splenium (arrow) of the corpus callosum. **H** Axial (4 mm/0.8 mm gap) and (**I**) coronal (2 mm/ 0 mm gap) turbo spin echo T2 weighted MR images show asymmetric lateral ventricles and caudate nuclei, with the body of the right caudate nucleus appearing slightly smaller than the left (arrow). **J** Axial spin echo 1.5 T Siemens Symphony T1 MR image (4 mm/ 0.8 mm gap) demonstrating the perisylvian cortex. The cortical architecture is not well assessed for MCD due to a combination of technical parameters and age-appropriate incompletely myelinated subcortical white matter. **K** Anterior coronal (2 mm/ 0 mm gap) turbo spin echo T2 weighted MR image shows interdigitating frontal lobes (arrows) attributed to deficiency of the falx cerebri. **L–P** MR images from Individual 3 at 7 years of age. **L** Midline reconstructed sagittal T1 MPRAGE MR image (0.8 mm/ 0 mm interslice gap) reveals accentuation of the usual thinning of the posterior body of the corpus callosum (arrow). **M** Axial T2 (4 mm/1.2 mm gap) and **N** coronal T1 MPRAGE (1.2 mm/0 mm gap) MR images show asymmetric lateral ventricles and caudate nuclei, with the body of the left caudate nucleus appearing smaller than the right (arrow). **O** Reformatted axial (0.8 mm thickness) and (**P**) direct coronal (1.2 mm/ 0 mm gap) T1 3D MPRAGE MR images demonstrate irregular, thickened perisylvian cortex, more pronounced on the right, consistent with polymicrogyria (arrows).

(HP:0025068) in which ocular misalignment varies with the direction of gaze. Congenital incomitant strabismus is rare, but it is possible that a subset of reported individuals with *TUBA1A*-associated strabismus had CFEOM.

Cyclic vomiting (HP:0002572) was reported in Individual 3 and has been reported previously in association with *TUBB3* p.(Glu410Lys) and *TUBB2B* p.(Cys354Arg), suggesting that this is a shared feature of certain tubulinopathies [14, 50]. The severity and frequency of cyclic vomiting in an individual with a *TUBB3* p.(Glu410Lys) variant was ameliorated by prophylactic valproic acid (VPA) treatment [14], and VPA has been used to successfully treat epilepsy in MCD patients who harbor *TUBA1A* or *TUBB2B* variants [48]. VPA may also be effective for individuals with *TUBA1A* variants who require intervention for cyclic vomiting.

CFEOM-associated variants in *TUBB3* and *TUBB2B* have been reported to stabilize MTs, and many alter kinesin binding and reduce MT-kinesin interactions [13, 15]. *TUBA1A*-CFEOM variants may also alter MT stabilization through changes in lateral (Arg156 and Gly59) or longitudinal interfaces (His406 and Met398), or through altered kinesin binding (His406). With a few exceptions, missense variants at specific β tubulin residues typically cause CFEOM while others cause MCD [13, 15, 16, 19]. Such a distinction in TUBA1A seems less clear. Since tubulinopathies are

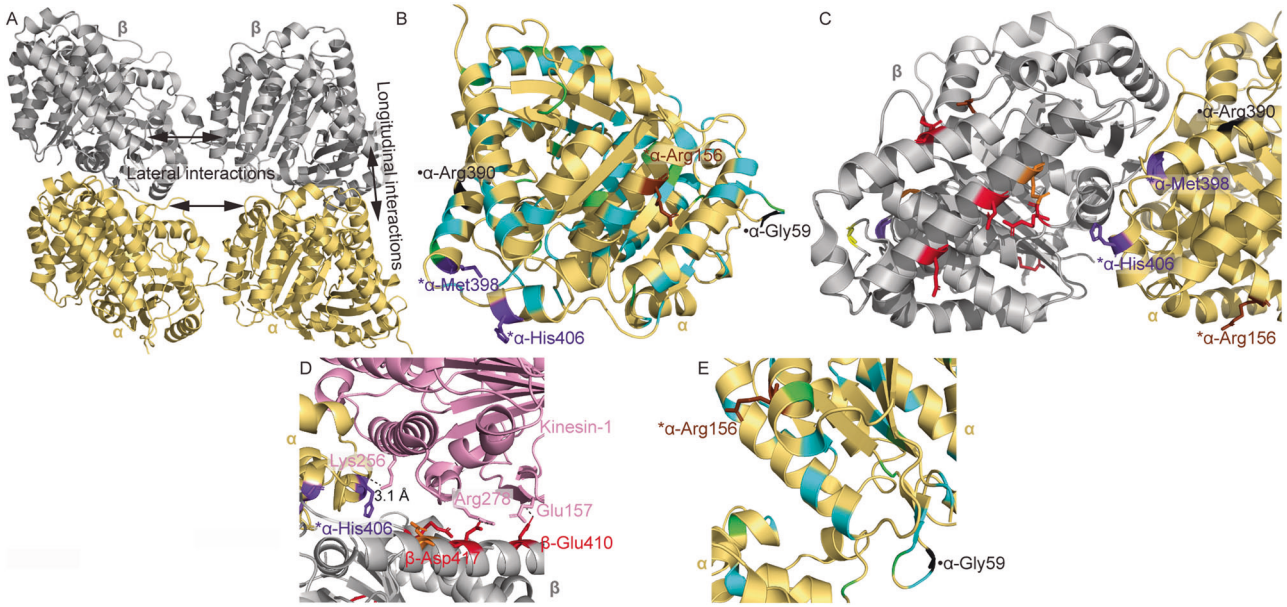

Fig. 3 Structural modeling of tubulinopathy variants. Structures were obtained from PDB ID: 3JAK (**A**–**C**, **E**) and PDB ID: 4HNA (D). **A** α and β tubulin monomers within a portion of a microtubule. Representative lateral and longitudinal interfaces are indicated. **B** α tubulin monomer with TUBA1A tubulinopathy-associated residues colored. **C** α and β tubulin monomers at the heterodimerization interface. Colored beta tubulin residues are associated with substitutions in TUBB3 and/or TUBB2B. For simplicity, residues associated with isolated MCD or MCD with involvement of cranial nerves other than CN3 are omitted in this view. **D** α and β tubulin complexed with kinesin-1. Colored beta tubulin residues are associated with substitutions in TUBB3 and/or TUBB2B. For simplicity, residues associated with isolated MCD or MCD with involvement of cranial nerves other than CN3 are omitted in this view. Polar interactions between kinesin and alpha or beta tubulin residues are shown with dashed lines. Distance between kinesin-Lys256 and α-His406 is shown. **E** Lateral interface between α tubulin residues in adjacent microtubule protofilaments. Key: α tubulin (gold); β tubulin (silver); kinesin-1 (pink); residues associated with CFEOM but not MCD (red); residues associated with CFEOM+MCD (purple); residues associated with MCD in the absence of CFEOM (cyan); residues associated with CFEOM ± MCD (orange); residues associated with CFEOM in the absence of MCD, or associated with MCD in the absence of CFEOM depending on substitution (brown); residues associated with MCD ± CFEOM (yellow); previously reported residues associated with putative CFEOM in the absence of MCD (black; [50]); reported residues associated with MCD and anomalies of cranial nerves other than CN III (green; [25]). *residues reported for the first time in this work (Arg156, Met398, and His406). ●-Previously reported residues associated with putative CN3 phenotypes [50].

associated with a broad spectrum of phenotypes which have been reported extensively [25, 48, 49], careful assessment and reporting of clinical features are advised.

In conclusion, this work demonstrates that distinct missense variants in *TUBA1A* result in CFEOM with or without MCD. Additional studies are warranted to elucidate the functional implications of specific *TUBA1A* missense variants. This report expands the genetic heterogeneity of CFEOM and suggests that screening of this additional tubulin-encoding gene should be pursued in patients with CFEOM with or without other findings who screen negative for variants in *KIF21A* and *TUBB3*.

Acknowledgements We thank the participants and their family members, Dr. Monkol Lek and Mr. Ben Weisburd for their efforts in reprocessing and upload of sequence data for analysis at the Broad Institute, and Dr. Dan Doherty of the University of Washington for connecting the Bostonian and Canadian researchers.

Funding This project was supported by NEI R01EY027421 and NHLBI X01HL132377 (ECE), the Broad Institute of MIT and Harvard Center for Mendelian Genomics (NHGRI/NEI/NHLBI UM1HG008900), the Ocular Genomics Institute Genomics Core (Massachusetts Eye and Ear Infirmary/Harvard Medical School, NEI 2P30EY014104), NHGRI R01HG009141, the Care4Rare Canada Consortium funded by Genome Canada and the Ontario Genomics Institute (OGI-147), the Canadian Institutes of Health Research, Ontario Research Fund, Genome Alberta, Genome British Columbia, Genome Quebec, and Children's Hospital of Eastern Ontario Foundation. JJ was supported by T32GM007748-42, 5T32NS007473-19, and 5T32EY007145-16. MW was supported by NEI 5K08EY027850 and BCH Ophthalmology Foundation Faculty Discovery Award. MW, SM, and DH receive research support from Children's Hospital Ophthalmology Foundation, Inc., Boston, MA. KMB is a Tier 1 Canada Research Chair in Rare Disease Precision Health. ECE is a Howard Hughes Medical Institute Investigator.

Compliance with ethical standards

Conflict of interest The authors declare that they have no conflict of interest.

Publisher's note Springer Nature remains neutral with regard to jurisdictional claims in published maps and institutional affiliations.

References

1. Lasser M, Tiber J, Lowery LA. The role of the microtubule cytoskeleton in neurodevelopmental disorders. Front Cell Neurosci. 2018;12:165.
2. Lopata MA, Cleveland DW. In vivo microtubules are copolymers of available beta-tubulin isotypes: localization of each of six vertebrate beta-tubulin isotypes using polyclonal antibodies elicited by synthetic peptide antigens. J Cell Biol. 1987;105:1707–20.
3. Tilney LG, Bryan J, Bush DJ, Fujiwara K, Mooseker MS, Murphy DB, et al. Microtubules: evidence for 13 protofilaments. J Cell Biol. 1973;59:267–75.
4. Mitchison T, Kirschner M. Dynamic instability of microtubule growth. Nature. 1984;312:237–42.
5. Fulton C, Simpson P. Selective synthesis and utilization of flagellar tubulin. The multi-tubulin hypothesis. Cell Motil. 1976;3:987–1005.
6. Gonçalves FG, Freddi T de AL, Taranath A, Lakshmanan R, Goetti R, Feltrin FS, et al. Tubulinopathies. Topics Magn Reson Imaging. 2018;27:395–408.
7. Köhler S, Carmody L, Vasilevsky N, Jacobsen J, Danis D, Gourdine J, et al. Expansion of the Human Phenotype Ontology (HPO) knowledge base and resources. Nucleic Acids Res. 2019;47:D1018–27.
8. Engle EC, Goumnerov BC, McKeown CA, Schatz M, Johns DR, Porter JD, et al. Oculomotor nerve and muscle abnormalities in congenital fibrosis of the extraocular muscles. Ann Neurol. 1997;41:314–25.
9. Demer JL, Clark RA, Engle EC. Magnetic Resonance Imaging Evidence For Widespread Orbital Dysinnervation in Congenital Fibrosis of Extraocular Muscles Due to Mutations in KIF21A. Invest Ophth Vis Sci. 2005;46:530–9.
10. Lim K, Engle E, Demer J. Abnormalities of the oculomotor nerve in congenital fibrosis of the extraocular muscles and congenital oculomotor palsy. Invest Ophth Vis Sci. 2007;48:1601–6.
11. Online Mendelian Inheritance in Man, OMIM. Mc-Kusick-Nathans Institute of Genetic Medicine, Johns Hopkins University (Baltimore, MD), accessed December 10, 2020. https://omim.org/
12. Yamada K, Andrews C, Chan W-M, McKeown CA, Magli A, Berardinis Tde, et al. Heterozygous mutations of the kinesin KIF21A in congenital fibrosis of the extraocular muscles type 1 (CFEOM1). Nat Genet. 2003;35:318–21.
13. Tischfield M, Baris H, Wu C, Rudolph G, Maldergem L, He W, et al. Human TUBB3 mutations perturb microtubule dynamics, kinesin interactions, and axon guidance. Cell. 2010;140:74–87.
14. Chew S, Balasubramanian R, Chan W, Kang P, Andrews C, Webb B, et al. A novel syndrome caused by the E410K amino acid substitution in the neuronal β-tubulin isotype 3. Brain. 2013;136:522–35.
15. Cederquist GY, Luchniak A, Tischfield MA, Peeva M, Song Y, Menezes MP, et al. An inherited TUBB2B mutation alters a kinesin-binding site and causes polymicrogyria, CFEOM and axon dysinnervation. Hum Mol Genet. 2012;21:5484–99.
16. Whitman MC, Andrews C, Chan W-M, Tischfield MA, Stasheff SF, Brancati F, et al. Two unique TUBB3 mutations cause both CFEOM3 and malformations of cortical development. Am J Med Genet A. 2016;170A:297–305.
17. Poirier K, Keays D, Francis F, Saillour Y, Bahi N, Manouvrier S, et al. Large spectrum of lissencephaly and pachygyria phenotypes resulting from de novo missense mutations in tubulin alpha1A (TUBA1A). Hum Mutat. 2007;28:1055–64.
18. Jaglin X, Poirier K, Saillour Y, Buhler E, Tian G, Bahi-Buisson N, et al. Mutations in the beta-tubulin gene TUBB2B result in asymmetrical polymicrogyria. Nat Genet. 2009;41:746–52.
19. Poirier K, Saillour Y, Bahi-Buisson N, Jaglin X, Fallet-Bianco C, Nabbout R, et al. Mutations in the neuronal ß-tubulin subunit TUBB3 result in malformation of cortical development and neuronal migration defects. Hum Mol Genet. 2010;19:4462–73.
20. Latremoliere A, Cheng L, DeLisle M, Wu C, Chew S, Hutchinson EB, et al. Neuronal-specific TUBB3 is not required for normal neuronal function but is essential for timely axon regeneration. Cell Rep. 2018;24:1865–79.e9.
21. Bittermann E, Abdelhamed Z, Liegel R, Menke C, Timms A, Beier D, et al. Differential requirements of tubulin genes in mammalian forebrain development. Plos Genet. 2019;15:e1008243–e1008243.
22. Keays D, Tian G, Poirier K, Huang G-J, Siebold C, Cleak J, et al. Mutations in alpha-tubulin cause abnormal neuronal migration in mice and lissencephaly in humans. Cell. 2007;128:45–57.
23. Furuse T, Yamada I, Kushida T, Masuya H, Miura I, Kaneda H, et al. Behavioral and neuromorphological characterization of a novel Tuba1 mutant mouse. Behavioural Brain Res. 2012;227:167–74.
24. Hanson MG, Aiken J, Sietsema DV, Sept D, Bates EA, Niswander L, et al. Novel α-tubulin mutation disrupts neural development and tubulin proteostasis. Dev Biol. 2016;409:406–19.
25. Hebebrand M, Hüffmeier U, Trollmann R, Hehr U, Uebe S, Ekici A, et al. The mutational and phenotypic spectrum of TUBA1A-associated tubulinopathy. Orphanet J Rare Dis. 2019;14:38–38.
26. Nellhaus G. Head circumference from birth to eighteen years. Pediatrics. 1968;41:106–14.
27. Li H, Durbin R. Fast and accurate short read alignment with Burrows-Wheeler transform. Bioinformatics. 2009;25:1754–60.
28. McKenna A, Hanna M, Banks E, Sivachenko A, Cibulskis K, Kernytsky A, et al. The Genome Analysis Toolkit: a MapReduce framework for analyzing next-generation DNA sequencing data. Genome Res. 2010;20:1297–303.
29. McLaren W, Gil L, Hunt SE, Riat HS, Ritchie GRS, Thormann A, et al. The ensembl variant effect predictor. Genome Biol. 2016;17:122.
30. Beaulieu CL, Majewski J, Schwartzentruber J, Samuels ME, Fernandez BA, Bernier FP, et al. FORGE Canada Consortium: outcomes of a 2-year national rare-disease gene-discovery project. Am J Hum Genetics. 2014;94:809–17.
31. Paila U, Chapman BA, Kirchner R, Quinlan AR. GEMINI: integrative exploration of genetic variation and genome annotations. Plos Comput Biol. 2013;9:e1003153.
32. Srour M, Schwartzentruber J, Hamdan F, Ospina L, Patry L, Labuda D, et al. Mutations in C5ORF42 cause Joubert syndrome in the French Canadian population. Am J Hum Genetics. 2012;90:693–700.
33. Lek M, Karczewski K, Minikel E, Samocha K, Banks E, Fennell T, et al. Analysis of protein-coding genetic variation in 60,706 humans. Nature. 2016;536:285–91.
34. Karczewski K, Francioli L, Tiao G, Cummings B, Alföldi J, Wang Q, et al. The mutational constraint spectrum quantified from variation in 141,456 humans. Nature. 2020;581:434–43.
35. Auton A, Abecasis GR, Altshuler DM, Durbin RM, Abecasis GR, Bentley DR, et al. A global reference for human genetic variation. Nature. 2015;526:68–74.
36. Landrum MJ, Lee JM, Benson M, Brown GR, Chao C, Chitipiralla S, et al. ClinVar: improving access to variant interpretations and supporting evidence. Nucleic Acids Res. 2018;46:D1062–7.
37. Zhang R, Alushin GM, Brown A, Nogales E. Mechanistic origin of microtubule dynamic instability and its modulation by EB proteins. Cell. 2015;162:849–59.
38. Gigant B, Wang W, Dreier B, Jiang Q, Pecqueur L, Plückthun A, et al. Structure of a kinesin–tubulin complex and implications for kinesin motility. Nat Struct Mol Biol. 2013;20:1001–7.
39. Sievers F, Wilm A, Dineen D, Gibson TJ, Karplus K, Li W, et al. Fast, scalable generation of high-quality protein multiple sequence alignments using Clustal Omega. Mol Syst Biol. 2011;7:539–539.

40. Waterhouse AM, Procter JB, Martin D, Clamp M, Barton GJ. Jalview Version 2—a multiple sequence alignment editor and analysis workbench. Bioinformatics. 2009;25:1189–91.
41. Shoshany T, Robson C, Hunter D. Anomalous superior oblique muscles and tendons in congenital fibrosis of the extraocular muscles. J Am Assoc Pediatr Ophthalmol Strabismus. 2019;23:325.e1–325.e6.
42. Pollard KS, Hubisz MJ, Rosenbloom KR, Siepel A. Detection of nonneutral substitution rates on mammalian phylogenies. Genome Res. 2010;20:110–21.
43. Rentzsch P, Witten D, Cooper G, Shendure J, Kircher M. CADD: predicting the deleteriousness of variants throughout the human genome. Nucleic Acids Res. 2019;47:D886–94.
44. Richards S, Aziz N, Bale S, Bick D, Das S, Gastier-Foster J, et al. Standards and guidelines for the interpretation of sequence variants: a joint consensus recommendation of the American College of Medical Genetics and Genomics and the Association for Molecular Pathology. Genet Med. 2015;17:405–23.
45. Samocha K, Robinson E, Sanders S, Stevens C, Sabo A, McGrath L, et al. A framework for the interpretation of de novo mutation in human disease. Nat Genet. 2014;46:944–50.
46. Nogales E, Whittaker M, Milligan RA, Downing KH. High-resolution model of the microtubule. Cell. 1999;96:79–88.
47. Löwe J, Li H, Downing KH, Nogales E. Refined structure of αβ-tubulin at 3.5 Å resolution. J Mol Biol. 2001;313:1045–57.
48. Romaniello R, Zucca C, Arrigoni F, Bonanni P, Panzeri E, Bassi MT, et al. Epilepsy in tubulinopathy: personal series and literature review. Cells. 2019;8:669.
49. Aiken J, Buscaglia G, Bates E, Moore J. The α-tubulin gene TUBA1A in brain development: a key ingredient in the neuronal isotype blend. J Dev Biol. 2017;5:8.
50. Romaniello R, Arrigoni F, Panzeri E, Poretti A, Micalizzi A, Citterio A, et al. Tubulin-related cerebellar dysplasia: definition of a distinct pattern of cerebellar malformation. Eur Radio. 2017;27:5080–92.

Affiliations

Julie A. Jurgens[1,2,3,4] · Brenda J. Barry[2,5] · Gabrielle Lemire[6] · Wai-Man Chan[1,2,3,4,5] · Mary C. Whitman[1,7,8] · Sherin Shaaban[1,2,3,9] · Caroline D. Robson[10,11] · Sarah MacKinnon[7,8] · Eleina M. England[12,13,14] · Hugh J. McMillan[15] · Christopher Kelly[16] · Brandon M. Pratt[1,2,3] · Care4Rare Canada Consortium · Anne O'Donnell-Luria[12,13,14] · Daniel G. MacArthur[12,13,17,18] · Kym M. Boycott[6,19] · David G. Hunter[7,8] · Elizabeth C. Engle[1,2,3,4,5,7,8]

1 F.M. Kirby Neurobiology Center, Boston Children's Hospital, Boston, MA, USA
2 Department of Neurology, Boston Children's Hospital, Boston, MA, USA
3 Department of Neurology, Harvard Medical School, Boston, MA, USA
4 Broad Institute of MIT and Harvard, Cambridge, MA, USA
5 Howard Hughes Medical Institute, Chevy Chase, MD, USA
6 Children's Hospital of Eastern Ontario Research Institute, University of Ottawa, Ottawa, ON, Canada
7 Department of Ophthalmology, Boston Children's Hospital, Boston, MA, USA
8 Department of Ophthalmology, Harvard Medical School, Boston, MA, USA
9 Department of Pathology, University of Utah School of Medicine, Salt Lake City, UT, USA
10 Division of Neuroradiology, Department of Radiology, Boston Children's Hospital, Boston, MA, USA
11 Department of Radiology, Harvard Medical School, Boston, MA, USA
12 Center for Mendelian Genomics, Program in Medical and Population Genetics, Broad Institute of MIT and Harvard, Cambridge, MA, USA
13 Analytic and Translational Genetics Unit, Massachusetts General Hospital, Boston, MA, USA
14 Division of Genetics and Genomics, Boston Children's Hospital, Boston, MA, USA
15 Division of Neurology, Department of Pediatrics, Children's Hospital of Eastern Ontario, Ottawa, ON, Canada
16 Pediatric Ophthalmology and Physician Informatics, MultiCare Health System, Tacoma, WA, USA
17 Centre for Population Genomics, Garvan Institute of Medical Research and UNSW, Sydney, NSW, Australia
18 Murdoch Children's Research Institute, Parkville, VIC, Australia
19 Department of Genetics, Children's Hospital of Eastern Ontario, Ottawa, ON, Canada